Int.J.Curr.Microbiol.App.Sci (2017) *6*(11): 1335-1350

International Journal of Current Microbiology and Applied Sciences
ISSN: 2319-7706 **Volume 6 Number 11 (2017) pp. 1335-1350**
Journal homepage: http://www.ijcmas.com

Original Research Article https://doi.org/10.20546/ijcmas.2017.611.160

Assessment of Cu- Chitosan Nanoparticles for its Antibacterial Activity against *Pseudomonas syringae pv. glycinea*

Swati*, Manju Kumari Choudhary, Arunabh Joshi and Vinod Saharan

Department of Molecular Biology and Biotechnology, Rajasthan College of Agriculture, Maharana Pratap University of Agriculture and Technology, Udaipur, Rajasthan, India
**Corresponding author*

Keywords

Cu-chitosan, Nanoparticles, Ionic gelation technique, Bacterial blight.

Article Info

Accepted:
12 September 2017
Available Online:
10 November 2017

A B S T R A C T

Bacterial Blight of Soybean is caused by the bacterial agent *Pseudomonas syringae pv. glycinea*. It attacks all of the above-ground parts of soybean. Use of agrochemicals, pesticides and phytochemicals leads the deterioration of soil health, degradation of agro-ecosystems and environment pollution. Chitosan NPs have been investigated as a carrier for active ingredient delivery for various applications due to their biocompatibility, biodegradability, high permeability, cost-effectiveness, non-toxicity and excellent film forming ability, antimicrobial and insecticidal activities. Different metal chitosan complexes have been prepared to improve antimicrobial activity of chitosan. Copper (Cu) compounds are well known for their biocide activity and it is essential for plant growth and development. Cu-chitosan NPs have remarkable potential and act as a highly effective antibacterial agent against Bacterial Blight of Soybean at the concentration of 400ppm and 1000ppm.

Introduction

Soybean [*Glycine max* (L.)] is one of the most important crop worldwide that provides two third of calories derived from agriculture (Ray *et al.*, 2013) and accounts for half of the global demand for oil and vegetable protein. Its continuous cultivation with simultaneous increase in area has led to increase in disease and pest occurrence. Currently, soybean is severely attacked by different major diseases, insect, pest and several weeds. Bacterial blight can be found in most soybean fields every year. Yield losses due to *Pseudomonas syringae pv. glycinea* have been reported as anywhere from 4%-40% depending on the severity of the conditions (Jagtap *et al.*, 2012). Bacterial blight of soybeans can enter leaves through wounds or natural openings such as stomata. After infection, small, water-soaked spots surrounded by a chlorotic halo appear on the leaves. The brown or black centers of these spots indicate that the tissue is dying. Typically these spots will enlarge and merge to form large, dead patches on the leaves.

The leaves appear ragged if the dead tissue falls out. Lesions on pods are initially small and water-soaked but eventually enlarge, turn brown to black, and merge to encompass the whole pod. Infection can also occur on the stems, petioles and seeds (Zou *et al.*, 2005). Agricultural production continues to be

challenged by a large number of insect pests, diseases and weeds accounting for 40% losses per year (Pimentel *et al.,* 2009). The use of chemical substances for controlling pathogen in soybean has been found to be effective (Allen *et al.,* 2004; Curto *et al.,* 2006; Brooker *et al.,* 2007) however long-term affect of pesticides might be vast and catastrophic on human beings, animals and soil micro-flora. Therefore, it should be regulated sincerely for protecting the ecosystem (Rai and Ingle, 2012).

Chitosan, a biopolymer of glucosamine and N-acetyl glucosamine residues, is a de-acetylated product of chitin. With the advancement of nanotechnology, chitosan based nanomaterials are being largely adapted for their exploration in plants (Shukla *et al.,* 2013).

Chitosan is able to chelate various organic and inorganic compounds, making it well-suited for improving the stability, solubility and biocidal activity of chelated fungicides or other pesticides (Shukla *et al.,* 2013).

Several studies showed that chitosan is not only an antimicrobial agent but also an effective elicitor of plant systemic acquired resistance to pathogens (Sharp *et al.,* 2013; Katiyar *et al.,* 2014; Xing *et al.,* 2014), enhancer and regulator of plant growth, development and yield (Gornik *et al.,* 2008; Cabrera *et al.,* 2013; Wang *et al.,* 2015).

Chitosan NPs reveal completely new or improved biological activities if compared with bulk chitosan due to altered physico-chemical characteristics like size, surface area, cationic nature, active functional groups, higher encapsulation efficiency etc (Saharan *et al.,* 2013). Chitosan NPs have been investigated as a carrier for active ingredient delivery for various applications due to their biocompatibility, biodegradability, high permeability, cost-effectiveness, non-toxicity and excellent film forming ability (Shukla *et al.,* 2013) antimicrobial and insecticidal activities (Yin *et al.,* 2010; Zeng *et al.,* 2012; Ma *et al.,* 2013; Chen *et al.,* 2014). Chitosan NPs treatment of leaves and seeds produced significant improvement in the plant growth and innate immune response through induction of defence enzyme activity, upregulation of defence related genes including that of several antioxidant enzymes as well as elevation of the levels of total phenolics (Chen *et al.,* 2014; Chandra *et al.,* 2015)

Different metal chitosan complexes have been prepared to improve antimicrobial activity of chitosan. Various metal ions like Ag^{+}, Cu^{2+}, Zn^{2+}, Mn^{2+}, or Fe^{2+} was individually loaded onto chitosan NPs for evaluation of antibacterial activity (Du *et al.,* 2009). Among these metals, Copper (Cu) compounds are well known for their biocide activity and it is essential for plant growth and development. Cu is also act as cofactor of numerous enzymes that take part in the electron transfer reactions of photosynthesis and respiration. In addition, Cu is involved in carbohydrate distribution, N_2 reduction and fixation, oxygen superoxide scavenging, ethylene sensing, cell wall metabolism, lignifications and protein synthesis. However, when Cu is present in high concentrations it is highly phytotoxic through interfering with photosynthesis, pigment synthesis and plasma membrane permeability. It causes metabolic disturbances that inhibit growth and development and initiate oxidative damage (Yruela *et al.,* 2009). Hence, Cu-chitosan complexes may serve as a reservoir for the slow release of Cu ions. The copper blending with chitosan have been developed to improve efficacy of their antibacterial (Qi *et al.,* 2004) and antifungal activities (Brunel *et al.,* 2013; Saharan *et al.,* 2013; Saharan *et al.,* 2015).

Materials and Methods

Synthesis of Cu-Chitosan NPs

For synthesis of Cu-chitosan NPs, a well-established and reproducible method of cross linking coupled with ultra-sonication was used as described earlier (Qi *et al.,* 2004; Du *et al.,* 2009; Corradini *et al.,* 2010; Fan *et al.,* 2012; Saharan *et al.,* 2013; Saharan *et al.,* 2015; Manikandan and Sathiyabama, 2016; Choudhary *et al.,* 2017). 0.1 gm of chitosan (low molecular weight and 80% N-deacetylation, Sigma-Aldrich, St.Louis, USA) mixed in 100 ml of 1% acetic acid and stirrer at 500- 550 rpm(for 30 minutes). 0.25 gm of TPP (Sodium tripolyphosphate anhydrous, Loba Chemie) mixed in 100 ml of deionized water and stirrer (Remi Laboratory Instruments, Mumbai, India) at 500- 550 rpm (for 30 minutes). Filter the solution using whatman qualitative filter paper-1. Then chitosan solution was stirrer at 500-550 rpm. TPP solution mixed in chitosan solution with dropping rate of about 40 drops/ minute (Fig. 1). Both solutions obtained as a colloidal solution. Before finishing cross linking reaction as described above, $CuSO_4$ solution (0.02 gm in 10 ml) added into formulation and kept it for overnight stirring. The pellet resulting from centrifuge was suspended in deionized water by using ultra sonication with (Qsonica Missonix, USA) for 120 sec. at 4°C. It was repeated three times and the precipitated pellet was lyophilized (Freeze dryer with concentrator, LabTech) and stored at 4°C for further use.

Characterization of Cu-chitosan NPs

Developed Cu-chitosan NPs were characterized for mean size, size distribution, functional group analysis and surface morphology by particle size analyzer (DLS: Dynamic Light Scattering), Fourier Transform Infra Red (FTIR), Transmission electron microscopy (TEM) and Scanning electron microscopy (SEM) through standardized methods (Saharan *et al.,* 2013; Saharan *et al.,* 2015). Elemental analysis of Cu-chitosan NPs was gauged by energy dispersive spectroscopy (SEM-EDS).

Dynamic light scattering (DLS) measurements

DLS was used for measurement of average particle size, polydispersity index (PDI) and zeta potential of nanoparticles on high performance particle zetasizer (ZS90, *Malvern, UK*). The sample was analyzed in triplicate at 25ºC at a scattering angle of 90°. Deionized water was used as a reference for dispersing medium. The results are given as the average particle size obtained from the analysis of three different batches, each of them measured three times.

Fourier transforms infrared (FTIR) analysis

To confirm the synthesis of various nanoparticles, FTIR analysis was done. The results were recorded by ALPHA FT-IR spectrometer combined with Quick Snap™ (Bruker, Germany). FTIR spectroscopy is based on the chemical bonds in a molecule that vibrate at characteristic frequencies depending on the elements and types of bonds. During FTIR measurements, a spot on the specimen is subjected to a modulated IR beam. The specimen's transmittance and reflectance of the infrared radiation at different frequencies is measured and translated into an IR absorption plot.

Transmission electron microscopy (TEM)

The nanocomposites were first diluted in ultrapure water (0.05 mg / ml, w/v), after which a negative staining technique was applied (Ottaviani *et al.,* 2000). In this technique, the diluted suspension was mixed with 2% uranyl acetate solution; a drop of the

mixture was deposited onto a standard copper grid covered by a holey carbon film and dried at ambient temperature before observation. TEM micrographs were obtained using a FEI Spirit TEM (Hillsboro, USA) operated at 120 kV using 400-mesh Formvar®carbon-coated copper grid.

Scanning electron microscopy (SEM) and energy dispersive X-ray spectroscope (EDS) observation

Scanning electron microscope was used to study the surface morphology of Cu-chitosan NPs. The samples were dried by critical point drying (CPD, *Emitech* K850) and mounted on aluminium stubs with double sided carbon and then coated with gold palladium using a sputter coater model SC7620 (*Emitech*). The images were then recorded in high vacuum mode using a Zeiss EVO MA10 scanning electron microscope (*Carl Zeiss Promenade*, Jena, Germany) between 400 X – 29.70 KX magnification at 20 kV EHT (Rejinolda *et al.*, 2011). Elemental analysis of nanoparticles were carried out by Zeiss EVOMA10 scanning electron microscope equipped with energy dispersive X-ray spectroscope elementary analyzer (EDS, *Oxford* Instruments) using analytical software QUANTAX 200.

Bacterial strain and inoculums preparation

Bacterial strain of *Pseudomonas syringae pv. glycinea* was obtained from Department of Pathology, Rajasthan College of Agriculture, Maharana Pratap University of Agriculture and Technology.

Growth medium

For the preparation of inoculums, a loopful of the stock culture were transfer in 50 ml of Luria Bertani broth and incubate at 37^0 C on shaker (120 rpm) a loopful of the stock culture was transfer in 50 ml of Luria Bertani broth and incubate at 370 C on shaker (120 rpm). OD was measured at 660 nm at various time durations (0, 12, 24, 36 and 48h). Then 100µl bacterial suspension were collected from appropriate growth inoculum and added to sterile test tubes containing LB Broth supplemented with different concentration of Cu-chitosan NPs viz. 100ppm, 400ppm, 600ppm and 1000ppm along with control (without treatment) Bulk controls (Cu and chitosan). Bacterial growth was assessed by measuring OD at 660nm at various time durations (0, 12, 24, 36 and 48 h). At appropriate growth of test sample, test sample were collected and serial diluted to achieve countable colony number.

Inoculation procedure

Further, 50 µl of diluted test sample was spread on 90 mm petri-plates containing King's medium B Base (King *et al.*, 1954). Colony numbers were counted after incubation of the plates for 24 hr in incubator at 29±1ºC. CFU/ ml were calculated using the equation given below-

$$\text{CFU} = \frac{\text{Colony no.}}{\text{Plated sample (ml)}} \text{ x dilution factor}$$

Results and Discussion

Synthesis of Cu-Chitosan NPs

Cu-chitosan NPs was prepared by interaction of TPP anion with cationic chitosan and further chelating of copper ions using ionic gelation method (Jaiswal *et al.*, 2012; Saharan *et al.*, 2015). Chitosan has inter and intra-molecular hydrogen bonding. Chitosan molecules in aqueous adopt extensive flexible structures due to the electrostatic repulsion between the chains. In diluted acetic acid, chitosan and TPP spontaneously formed dense micro-nano complex. Under specific intensity of ultrasonic waves, cavitations generated by ultrasonication reorganize the

complex and convert the micro complex into nano complex. Cu-chitosan NPs prepared in the present study exhibit a white crystal powder and appeared a semitransparent colloidal in aqueous. Cu-chitosan NPs were prepared by the interaction of oppositely charged macromolecules (chitosan and TPP) using ionic gelation method (Qi *et al.*, 2004; Du *et al.*, 2009; Corradini *et al.*, 2010; Fan *et al.*, 2012; Saharan *et al.*, 2013; Saharan *et al.*, 2015; Manikandan and Sathiyabama, 2016).

Characterization of Cu-chitosan NPs

DLS was used for the measurement of mean particles size, polydipersity index (PDI) and zeta potential of Cu-chitosan NP. The size distribution profile, shown in Figure 2A, represents mean hydrodynamic diameter of Cu-chitosan NP, 295.4 ± 2.8nm. The PDI value 0.28 indicated monodisperse nature of Cu-chitosan NP. Zeta potential of Cu-chitosan NP (+ 19.6 mV, Fig. 2B) showed overall positive charge, which is important parameter for the stability and higher affinity towards biological membranes (Qi *et al.*, 2004; Du *et al.*, 2009; Saharan *et al.*, 2013; Saharan *et al.*, 2015). In present study, mean hydrodynamic diameter of Cu-chitosan NPs was 295.4 nm. The lower PDI value (0.28) specified the monodisperse nature of Cu-chitosan NP.

In present study, + 19.6 mV zeta potential was recorded, which indicate overall positive charge on the surface of NPs. The positive zeta potential significantly influences particle stability in suspension through the electrostatic repulsion between the positively charged nanoparticles. Thus the nanoparticles remain separated in the suspension and formulation become stable. In addition, positively charged nanoparticles have more affinity towards the negatively charged biological membranes. Therefore nanoparticles express more biological interaction in living system. It also signifies for more antimicrobial activities (Qi *et al.*, 2004; Du *et al.*, 2009; Saharan *et al.*, 2013; Saharan *et al.*, 2015). Charged nanoparticles have been reported to induce the foundation of new and longer pore by interacting with negatively charged macromolecules of biological membranes of fungi and bacteria, thus act as strong antimicrobial agents.

Table.1 Elemental analysis of Cu-chitosan NP

Elements	At porous spot		At non porous spot	
	Weight %	Atomic %	Weight %	Atomic %
C	54.43	63.02	43.75	52.78
O	30.19	26.24	35.15	31.83
P	6.19	2.78	9.8	4.58
N	7.69	7.63	10.20	10.55
Cu	1.51	0.33	1.09	0.25
Totals	100.00			

Table.2

Treatment	CFU/ml
Control	103
Bulk	146
CuSo4	63.2
100 ppm	102
400ppm	5
600ppm	14
1000ppm	0

Fig.1 Scale up synthesis of Cu-chitosan nanoparticles

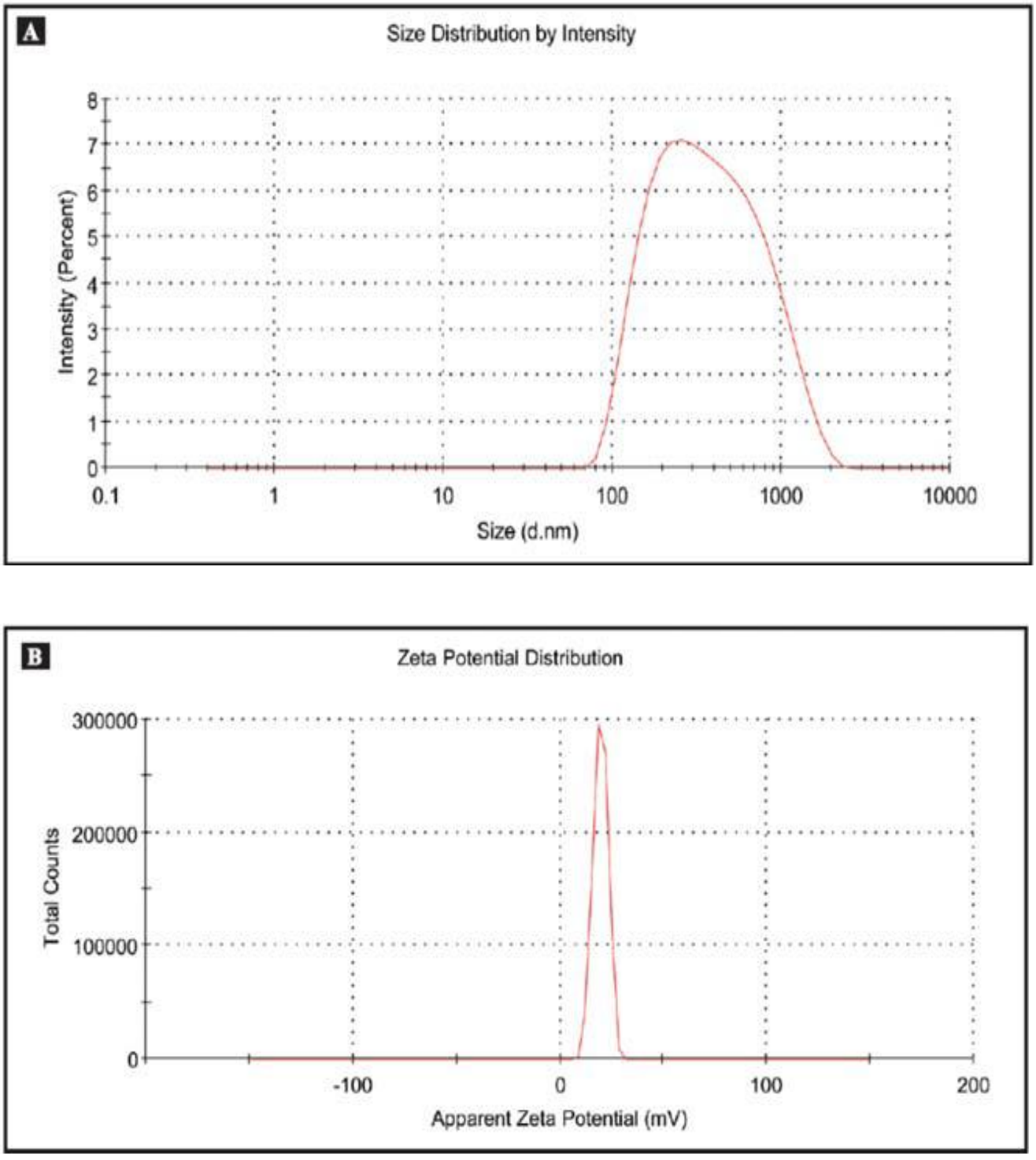

Fig.2 DLS analysis of Cu-chitosan NPs (A) Size distribution by intensity and (B) Zeta potential distribution

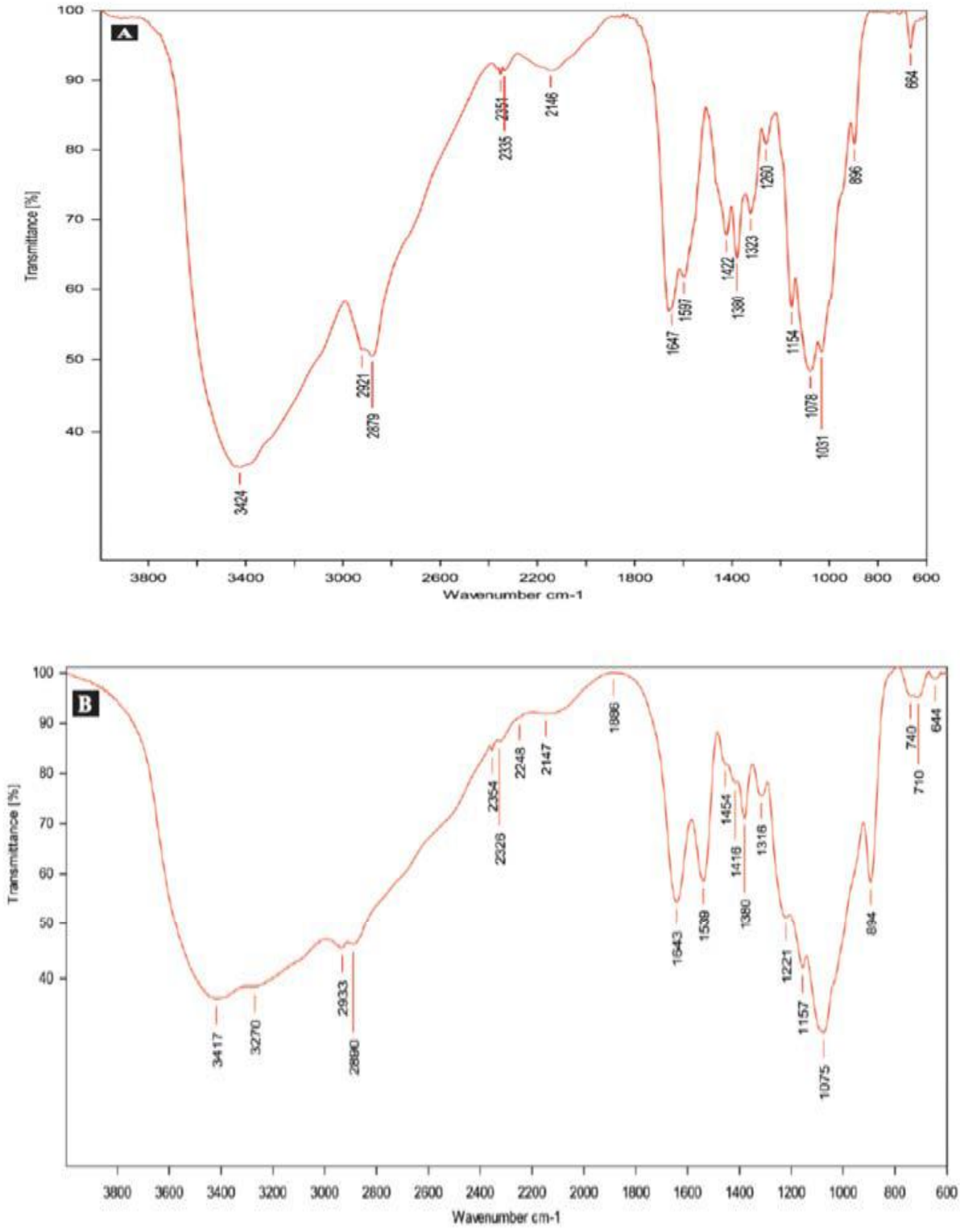

Fig.3 FTIR spectra (A) Bulk chitosan and (B) Cu-chitosan NPs

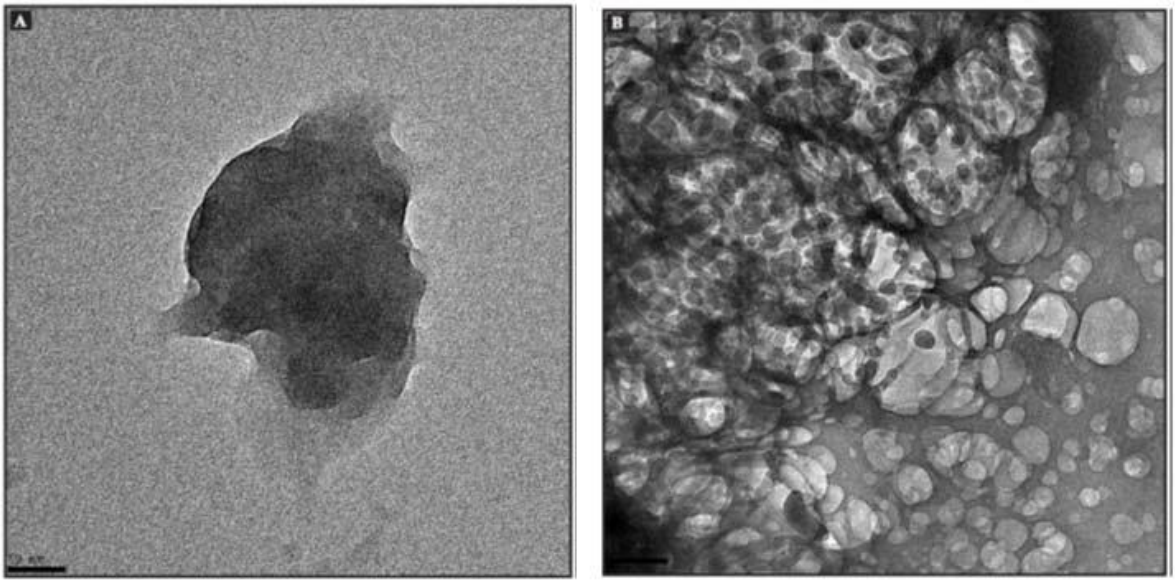

Fig.4 TEM images of (A) Sphere shaped Cu-chitosan NCPs and (B) Porous Cu-chitosan NPs.

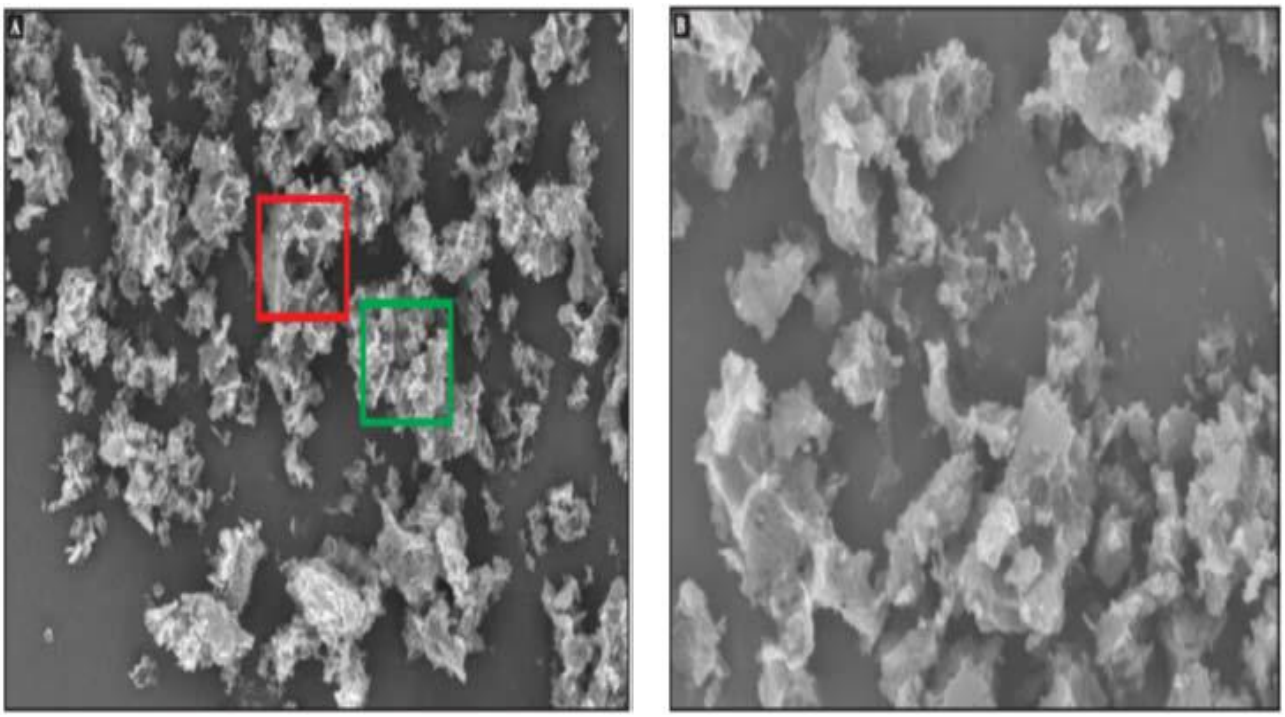

Fig.5 SEM micrographs (A) Cu-chitosan NCPs at 9.2mm ×1.00K and (B) Porous Cu chitosan at 9.2mm ×3.00K revealed nano (in green rectangular) and micro size pores (in red rectangular)

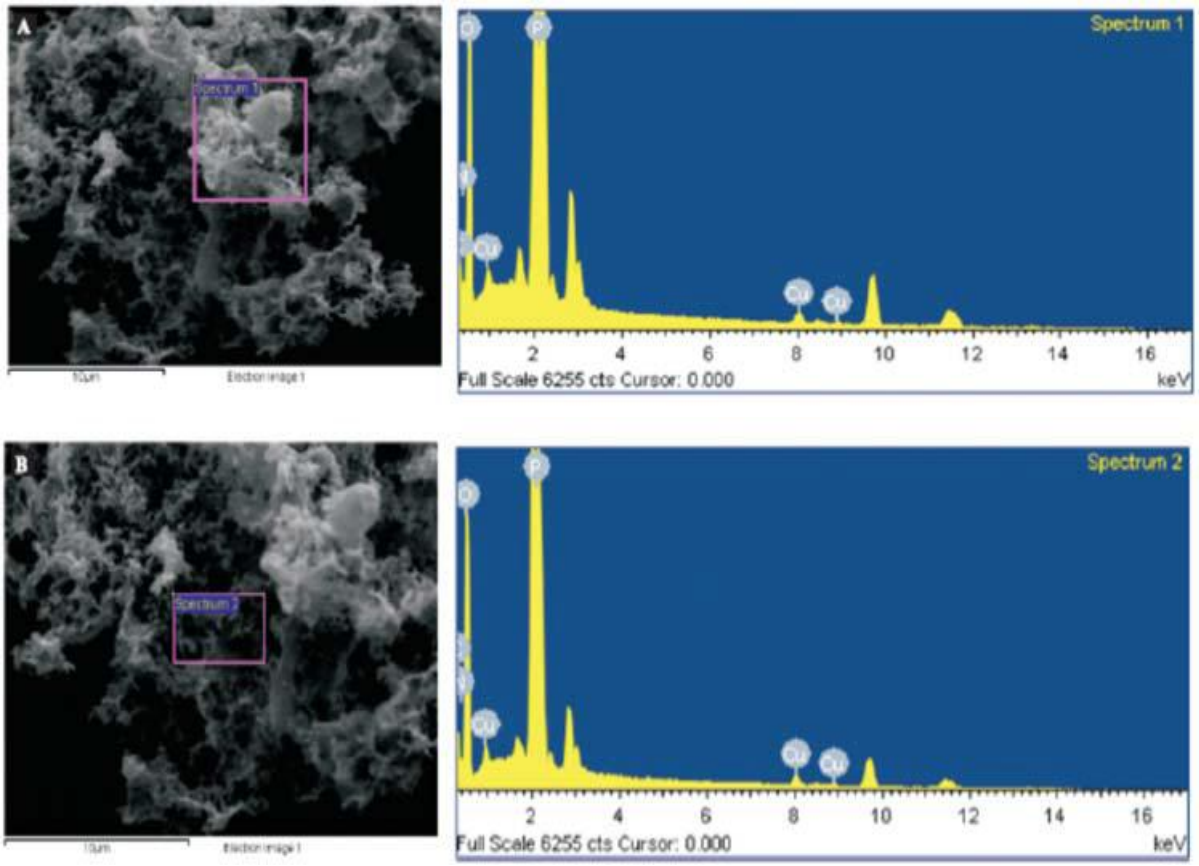

Fig.6 SEM-EDS elemental analysis of Cu-chitosan NCPs (A) Spectra of non-porous surface and (B) porous surface.

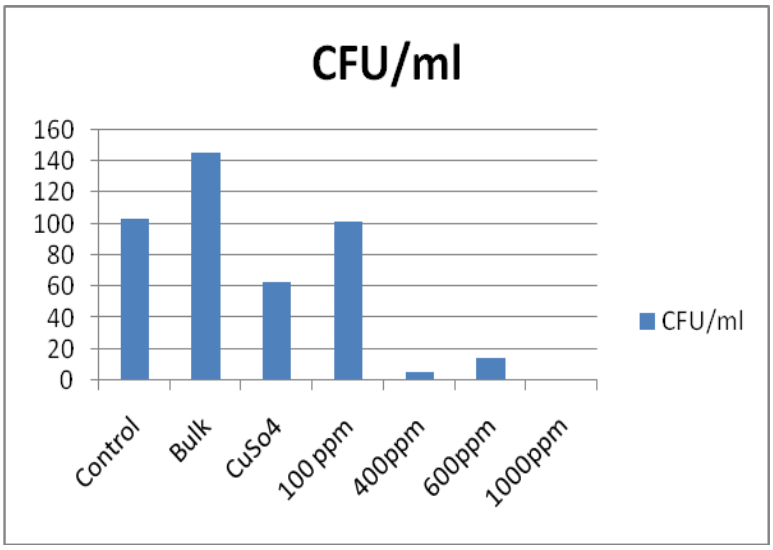

Fig.7 Effect of Cu-chitosan NPs on bacterial colony forming units

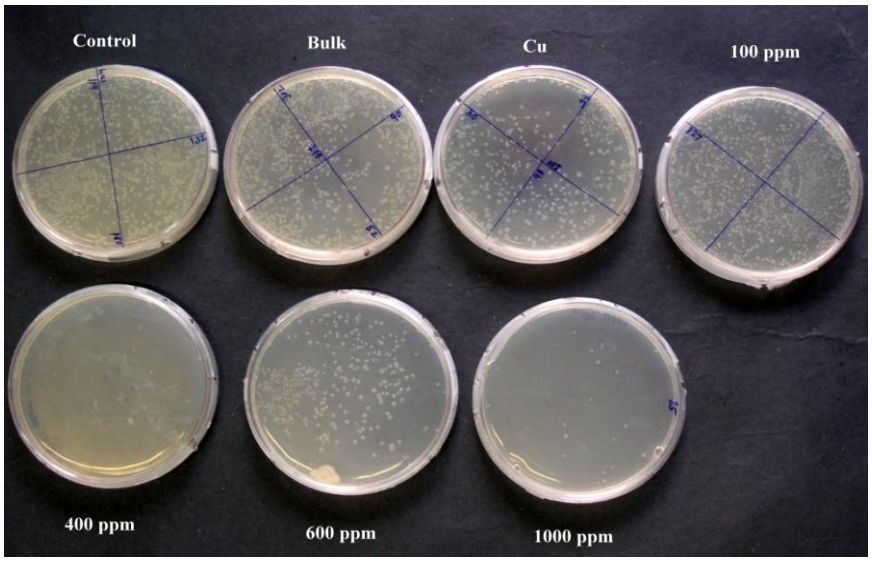

Fig.8 Antibacterial activity of different concentrations of Cu-chitosan NPs (100, 400, 600 and 1000ppm) with control, bulk chitosan and Cu against *in vitro* bacterial colony number of *Pseudomonas syringae pv. glycinea.*

Fourier Transforms Infrared (FTIR) Analysis

FTIR analysis was performed to confirm the interaction of chitosan, TPP and Cu. In bulk chitosan a specific peak at 3424 cm^{-1} corresponds to the combined peaks of the -NH_2 and -OH group stretching vibration. The band at 1647cm^{-1} is attributed to the CO-NH_2 group. The 1597 cm^{-1} peak of the -NH_2 bending vibration is sharper than the peak at 1647 cm^{-1}, which shows the high degree of deacetylation of the chitosan (Fig. 3A). The peaks at 1647 cm^{-1} (-$CONH_2$) and 1597 cm^{-1} (-NH_2) in the spectrum of Cu - chitosan NP was sharper and shifted to 1643 and 1539 cm^{-1}. Therefore, Cu interaction with chitosan induces redistribution of vibration frequencies (Fig. 3B). FTIR spectroscopy used infra-red waves which induce vibration in the chemical bonds and due to this vibration the presence and absence of functional group in sample could be examined. In present study, FTIR analysis was performed to confirm the interaction of chitosan, TPP and Cu. In bulk chitosan specific peaks at 3424 cm^{-1} and 1647cm^{-1}corresponds to the combined peaks of the -NH_2, -OH group stretching vibration and CO-NH_2 group were observed. In Cu - chitosan NP spectrum, the peaks at 1647 cm^{-1} (-$CONH_2$) and 1597 cm^{-1} (-NH_2) were sharper and shifted to 1643 and 1539 cm^{-1}. Therefore, FTIR study showed redistribution of vibration frequencies in Cu-chitosan NP in compared to bulk chitosan and these results were in line with earlier findings (Saharan *et al.,* 2013; Saharan *et al.*, 2015; Choudhary *et al.,* 2017).

TEM and SEM analyses

Actual behaviour of nanoparticles in aqueous suspension comes only through TEM study. Sphere-shaped (Fig. 4A) NP along with network of pores (Fig. 4B) verified by TEM. Further nano-organization of Cu-chitosan NP was confirmed by SEM micrograph. Cu-chitosan NP possess homogenous crystalline morphology at lower magnification (Fig. 5A). Whereas, highly porous structure (like barred enclosure) was displayed at higher magnification. Micro and nanoscale size pores were observed as per SEM micrograph

(Fig. 5B). TEM micrograph confirmed the nano-orgnization of synthesized materials. Spherical shaped Cu-chitosan NP in range of 100-500 nm was observed under TEM study. TEM results obtained in present study, was found similar to earlier report, where Cu-chitosan NP showed highly porous network of chitosan nanomaterials (Saharan *et al.,* 2015).

SEM-Energy Dispersive X-ray Spectroscopy (EDS) Analysis

In addition to SEM, energy-dispersive X-ray spectroscopies (EDS) of different spots on the samples were taken for determining the elemental composition of Cu-chitosan NP. Energy dispersive X-ray spectroscopy analysis revealed the presence of chitosan+ TPP (as C, O, P and N) and Cu in the NP (Fig. 6A and B; Table 1). EDS analysis at porous surface of Cu-chitosan NP as shown more Cu deposition compared to spectra of non porous surface. EDS study confirmed the presence of chitosan and Cu in the prepared NP. In present study SEM micrograph of Cu-chitosan NP elucidate well organized spongy porous surface at 9.2mm ×1.00K (Jaiswal *et al.,* 2012). Presence of Cu in chitosan NP was confirmed by SEM-EDS. EDS spectra at porous and non-porous surface of chitosan NPs manifest higher and lower Cu deposition. In present study EDS spectrum undoubtedly explain the mechanism described earlier (Qi *et al.,* 2004), in which Cu sorption could be understand by ion-exchange resins and surface chelating into porous nanomaterials.

Antibacterial activity

The tasted Cu-chitosan NPs differ in concentration of Cu-chitosan and Cu content. Concentration 1000ppm of Cu-chitosan NPs is more effective followed by 400ppm and 600ppm concentrations against *Pseudomonas syringae pv. glycinea*. 100ppm concentrations show lowest antibacterial activity (Fig. 7, 8 and Table 2).

Acknowledgments

Authors appreciate Nano Research Facility (NRF), Washington University in St. Louis for TEM analysis. Authors also acknowledge SEMF, Division of Entomology, IARI, New Delhi and SICART, Vallabh Vidyanagar, Anand, Gujarat for SEM analysis.

References

Abhilash, P.C. and Singh, N. 2009. Pesticide use and application: an Indian scenario. Journal of Hazardous Materials, 165: 1-12.

Allen, T.W., Enebak, S.A. and Carey, W.A. 2004. Evaluation of fungicides for control of species of *Fusarium* on long leaf pine seed. Crop Protection, 23: 979-982.

Anusuya, S. and Sathiyabama, M. 2014. Preparation of β-d-glucan nanoparticles and its antifungal activity. International Journal of Biological Macromolecules, 70: 440-443.

Brooker, N.L., Lagalle, C.D., Zlatanic, A., Javni, I. and Petrovic, Z. 2007. Soy polyol formulations as novel seed treatments for the management of soil-borne diseases of soybean. Communications in agricultural and applied biological sciences, 72(2): 35-43.

Brunel, F., Gueddari, N.E.E. and Moerschbacher, B.M. 2013. Complexation of copper (II) with chitosan nanogels: Toward control of microbial growth. Carbohydrate Polymers, 92: 1348-1356.

Buzea, C.P.I. and Robbie, K. 2007. Nanomaterials and nanoparticles: Sources and toxicity. Biointerphases, 2(4): 17-71.

Cabrera, J.C., Wégria, G., Onderwater, R.C.A., González, G., Nápoles, M.C., Falcón-Rodríguez, A.B., Costales, D.,

Rogers, H.J., Diosdado, E., González, S., Cabrera, G., González, L. and Wattiez, R. In: S. Saa Silva, *et al.*, (Eds.), 2013. Proc. 1st World Congresson the Use of Biostimulants in Agriculture, Acta Horticultural, 1009 ISHS.

Chandra, S., Chakarborty, N., Dasgupt, A., Sarkar, J., Panda, K. and Acharya, K. 2015. Chitosan nanoparticle: A positive modulator of innate immune responses in plants. Scientific Reports, 5: 1-13.

Chen, J., Zou, X., Liu, Q., Wang, F., Feng, W. and Wan, W. 2014. Combination effect of chitosan and methyl jasmonate on controlling *Alternaria alternata* and enhancing activity of cherry tomato fruit defense mechanisms. Crop Protection, 56: 31-36.

Choudhary, MK., Swati and Saharan, V. 2017. Synthesis, characterization and evaluation of physico-chemical profile of Cu-Chitosan Nanocomposite. International Journal of Chemical Studies, 5(4): 1489-1494.

Curto, G., Lazzeri L., Dallavalle E., Santi R. and Malaguti L. 2006. Effectiveness of crop rotation with *Brassicaceae* species for the management of the southern root-knot nematode *Meloidogyne incognita*. In: Abstracts 2nd International Biofumigation Symposium, June 25-29, Moscow, Idaho: pp 51.

Dhoke, S.K., Mahajan, P., Kamble, R. and Khanna, A. 2013. Effect of nanoparticles suspension on the growth of mung (*Vigna radiata*) seedlings by foliar spray method. Nanotechnological Development, 3(1): 1-7.

Dimkpa, C.O., McLean, J.E., Latta, D.E., Manango´n, E., Britt, D.W., Johnson, W.P., Boyanov, M.I. and Anderson, A.J. 2012. CuO and ZnO nanoparticles: phytotoxicity, metal speciation and induction of oxidative stress in sand-grown wheat. Journal of Nanoparticle Research, 14: 11-25.

Du, W.L., Niu, S.S., Xu, Y.L., Xu, Z.R. and Fan, C.L. 2009. Antibacterial activity of chitosan tripolyphosphate nanoparticles loaded with various metal ions. Carbohydrate Polymers, 75: 385-389.

Fisher, M.C., Henk, D.A., Briggs, C.J., Brownstein, J.S., Madoff, L.C., McCraw, S.L. and Gurr, S.J. 2012. Emerging fungal threats to animal, plant and ecosystem health. *Nature*, 484: 186-194.

Gogos, A., Knauer, K. and Bucheli, T.D. 2012. Nanomaterials in plant protection and fertilization: current state, foreseen applications, and research priorities. Journal of Agricultural and Food Chemistry, 60(39): 9781-9792.

Gornik, K. Grzesik, M. and Duda B. R. 2008. The effect of chitosan on rooting of gravevine cuttings and on subsequent plant growth under drought and temperature stress. Journal of Fruit and Ornamental Plant Resources, 16: 333-343.

Hadwiger, L.A. 2013. Multiple effects of chitosan on plant systems: Solid science or hype. Plant Science, 208: 42-49.

He, L., Liu, Y., Mustapha, A. and Lin, M. 2011. Antifungal activity of zinc oxide nanoparticles against *Botrytis cinerea* and *Penicillium expansum*. Microbiological Research, 166: 207-215.

Jagtap, Dhopte and Dey, June 2012. "Bio-efficacy of different antibacterial antibiotic, plant extracts and bioagents against bacterial blight of soybean caused by *Pseudomonas syringae* pv. glycinea". Scientific Journal of Microbiology.

Jaiswal M, Chauhan D, Sankararama Krishnan N. 2012. Copper chitosan nanocomposite: synthesis, characterization, and application in

removal of organophosphorous pesticide from agricultural runoff. Environmental Science Pollution Research; 19:2055-2062.

Jayaseelan, C., Ramkumar, R., Rahuman, A.A. and Perumal, P. 2013. Green synthesis of gold nanoparticles using seed aqueous extract of *Abelmoschus esculentus* and its antifungal activity. Industrial Crops and Products, 45: 423-429.

Jo, Y.K., Kim, B.H. and Jung, G. 2009. Antifungal activity of silver ions and nanoparticles on phytopathogenic fungi. Plant Disease, 93: 1037-1043.

Kaewnum, S., Prathuangwong, S. and Burr, T. J. 2005. Aggressiveness of *Xanthomonas axonopodis* pv. *glycines* isolates to soybean and hypersensitivity responses by other plants. Plant Pathology, 54: 409-415.

Kah, M., Tiede, K., Beulke, S. and Hofmann, T. 2013. Critical Reviews in Environmental Science and Technology, 43: 1823-1867.

Katiyar, D., Hemantaranjan, A., Singh, B. and Bhanu, A.N. 2014. A Future Perspective in Crop Protection: Chitosan and its Oligosaccharides. Advances in Plants & Agriculture Research, 1(1): 00006.

Khot, L., Sankaran, S., Maja, J., Ehsani, R. and Schuster, E.W. 2012. Application of nanomaterial in agricultural production and crop production: A review. Journal of Crop Protection, 35: 64-70.

Kim, K.J., Sung, W.S., Suh, B.K., Moon, S.K., Choi, J.S., Kim, J.G. and Lee, D.G. 2009. Antifungal activity and mode of action of silver nano-particles on *Candida albicans*. Biometals, 22(2): 235-242.

Kim, S.W., Jung, J.H., Lamsal, K., Kim, Y.S., Min, J.S. and Lee, Y.S. 2012. Antifungal effects of silver nanoparticles (AgNPs) against various plant pathogenic fungi. Mycobiology, 40(1): 53-58.

Kohler, H.R. and Triebskorn, R. 2013. Wildlife ecotoxicology of pesticides: can we track effects to the population level and beyond? Science, 341: 759-65.

Kolandasamy, M. and Ponnusamy, P. 2013. Expression of phenolics and defence related enzymes in relation to red root rot disease of tea plants. Archives of Phytopathology and Plant Protection, 46 (4): 451-462.

Kumari, M., Mukherjee, A. and Chandrasekaran, N. 2009. Genotoxicity of silver nanoparticles in *Allium cepa*. Science of the Total Environment, 407: 5243-5246.

Lamsal, K., Kim, S.W., Jung, J.H., Kim, Y.S., Kim, K.S. and Lee, Y.S. 2011. Inhibition effects of silver nanoparticles against powdery mildews on Cucumber and Pumpkin. Mycobiology, 39 (1): 26-32.

Lin, D. and Xing, B. 2008. Root uptake and phytotoxicity of ZnO nanoparticles. Environmental Science and Technology, 42: 5580-5582.

Ma, C., Chhikara, S., Xing, B., Musante, C., White, J.C. and Dhankher, O.P. 2013. Physiological and molecular response of *Arabidopsis thaliana* (L.) to nanoparticle cerium and indium oxide exposure. *ACS Sustain.* Chemical Engineering 1: 768-778.

Mahajan, P. Dhoke, S.K. and Khanna, A.S. 2011. Effect of nano-ZnO particle suspension on growth of mung (*Vigna radiata*) and gram (*Cicer arietinum*) seedlings using plant agar method. Journal of Nanotechnology, 2011: 1-7.

Mittler, R. 2002. Oxidative stress, antioxidants and stress tolerance. Trends in Plant Science, 7(9): 405-410.

Nair, R., Varghese, S.H., Nair, B.G.,

Maekawa, T., Yoshida, Y. and Sakthi K. D. 2010. Nanoparticulate material delivery to plants. Plant Science, 179: 154-163.

Narvel, J.M., Jakkula, L.R., Phillips, D.V., Wang, T., Lee, S-H. and Boerma, H.R. 2001. Molecular mapping of *Rxp* conditioning reaction to bacterial pustule in soybean. Journal of Heredity, 92: 267-70.

Park, H.J., Kim, S.H., Kim, H.J. and Choi, S.H. 2006. A new composition of nanosized silica-silver for control of various plant diseases. Plant Pathology Journal, 22: 295-302.

Pereira, P., Ibanez, S.G., Agostini, E. and Etcheverry, M. 2011. Effects of maize inoculation with *Fusarium verticillioides* and with two bacterial biocontrol agents on seedlings growth and antioxidative enzymatic activities. Applied Soil Ecology, 51: 52-59.

Perez-de-Luque, A., Cifuentes, Z., Beckstead, J.A., Sillero, J.C., Anila, C., Rubio, J. and Ryan, R.O. 2012. Effect of amphotericin B nanodisks on plant fungal disease. Pest Management Science, 68: 67-74.

Pimentel, D. 2009. The science of global challenge. Chapter 15: Pesticide and world food supply. ACS Symposium Series, 483: 309-323.

Qi, L., Xu, Z., Jiang, X., Hu, C. and Zou, X. 2004. Preparation and antibacterial activity of chitosan nanoparticles. Carbohydrate Research, 339(16): 2693-2700.

Rai, M. and Ingle, A. 2012. Role of nanotechnology in agriculture with special reference to management of insect pests. Applied Microbiology and Biotechnology, 94: 287-293.

Ray, D.K., Mueller, N.D., West P.C. and Foley J.A. 2013. Yield trends are insufficient to double global crop production by 2050, Proceeding of National Academy of Science, 8: 66428.

Saharan, V., Khatik, R., Choudhary, M.K., Mehrotra, A., Jakhar, S., Raliya, R., Nallamuthu, I. and Pal, A. 2014. Nano-materials for plant protection with special reference to Nano chitosan, *In: proceedings of 4th Annual International conference on Advances in Biotechnology*, GSTF, Dubai, pp 23-25.

Saharan, V., Mehrotra, A., Khatik, R., Rawal, P., Sharma, S.S. and Pal, A. 2013. Synthesis of chitosan based nanoparticles and their in vitro evaluation against phytopathogenic fungi. International journal of Biological Macromolecules, 62: 677-683.

Saharan, V., Sharma, G., Yadav, M., Choudhary, M.K., S.S. Sharma, Pal, P., Raliya, R. and Biswas, P. 2015. Synthesis and *in vitro* antifungal efficacy of Cu–chitosan nanoparticles against pathogenic fungi of tomato. International journal of Biological Macromolecules, 75: 346-353.

Sasson, Y., Levy-Ruso, G., Toledano, O. Ishaaya, I. in: I. Ishaaya, R. Nauen, A.R.Horowitz (Eds.), 2007. Insecticides Design Using Advanced Technologies, Springer-Verlag, Netherlands, pp. 1–32.

Sen, I.K., Mandal, A.K., Chakraborti, S., Dey, B., Chakraborty, R. and Islam, S.S. 2013. Green synthesis of silver nanoparticles using glucan from mushroom and study of antibacterial activity. International journal of Biological Macromolecules, 62: 439-449.

Sharon, M., Choudhary, A. and Kumar, R. 2010. Nanotechnology in agricultural diseases and food safety. Journal of Phytology, 2: 83-92.

Sharp, R.G. 2013. A Review of the Applications of Chitin and Its Derivatives in Agriculture to Modify

Plant-Microbial Interactions and Improve Crop Yields. Agronomy, 3: 757-793.

Shukla, K.S., Mishra, A.K., Arotiba, O.A. and Mamba, B.B. 2013. Chitosan-based nanomaterials: A state-of-the-art review. International Journal of Biology and Macromolecules, 59: 46-58.

Thuesombat, P., Hannongbua, S., Akasit, S. and Chadchawan, S. 2014. Effect of silver nanoparticles on rice (*Oryza sativa L.* cv. *KDML 105*) seed germination and seedling growth. Ecotoxicology and Environmental Safety, 104: 302-309.

Wang, X.H., Du, Y.M. and Liu, H. 2004. Preparation, characterization and antimicrobial activity of chitosan-Zn complex. Carbohydrate Polymers, 56: 21-26.

Wani, I.A. and Ahmad, T. 2013. Size and shape dependant antifungal activity of gold nanoparticles: A case study of Candida. Colloids and Surfaces B: Biointerfaces, 101: 162-170.

Wrather, J.A., Anderson, T.R., Arsyad, D.M., Tan, Y., Ploper, L.D., Porta-Puglia, A., Ram, H.H. and Yorinori, J.T., 2001. Soybean disease loss estimates for the top ten soybean-producing countries in 1998. Canadian Journal of Plant Pathology, 23: 115-121.

Xing, K., Zhu, X., Peng, X. and Qin, S. (2014). Chitosan antimicrobial and eliciting properties for pest control in Agricultural: A review. Agronomy of Sustainable Development, 35(2): 569-588.

Yin, H., Zhao, X. and Du, Y. 2010. Oligochitosan: A plant diseases vaccine-A review. Carbohydrate Polymer, 82: 1-8.

Yruela, I. 2009. Copper in plants: acquisition, transport and interactions. Functional Plant Biology, 36: 409-430.

Zeng, D. and Luo, X. 2012. Physiological effects of chitosan coating on wheat growth and activities of protective enzyme with drought tolerance. Open Journal of soil science, 2: 282-288.

Zou, J., Rodriguez-Zas, S., Aldea, M., Li, M., Zhu, J., Gonzalez, DO. 2005. Expression Profiling Soybean Response to *Pseudomonas syringae* Reveals New Defense-Related Genes and Rapid HR-Specific Downregulation of Photosynthesis. Molecular Plant-Microbe Interactions, 18(11): 1161-1174.

How to cite this article:

Swati, Manju Kumari Choudhary, Arunabh Joshi and Vinod Saharan. 2017. Assessment of Cu-Chitosan Nanoparticles for its Antibacterial Activity against *Pseudomonas syringae pv. glycinea*. *Int.J.Curr.Microbiol.App.Sci.* 6(11): 1335-1350.
doi: https://doi.org/10.20546/ijcmas.2017.611.160